Very-low-frequency saucers observed on DEMETER

H. Gordon James, Michel Parrot, Jean-Jacques Berthelier

Very-low-frequency saucers observed on DEMETER

H. G. James,[1] M. Parrot,[2] and J.-J. Berthelier[3]

Received 18 May 2012; revised 30 July 2012; accepted 2 August 2012; published 14 September 2012.

[1] Observations of very-low-frequency saucers by the electric field instrument (Instrument Champ Electrique, ICE) aboard the DEMETER spacecraft have added new evidence about the nature of the highly localized source of this radiation. DEMETER orbited sun-synchronously at altitudes around 660 km, significantly below those at which earlier spacecraft detected saucers. Also, DEMETER data establish the existence of saucer sources in the dayside ionosphere. Frequency-time slopes of saucers in DEMETER spectrograms have been analyzed with two-dimensional ray tracing. To produce such slopes requires long vertical separations between the source and the spacecraft, in some cases much greater than the height of the spacecraft above ground. It is concluded that the sources lie above the satellite and radiate downward. Bidirectional radiation patterns and the broadband quasielectrostatic whistler mode energy spectrum are consistent with the published results of simulations of nonlinear two-stream instabilities.

Citation: James, H. G., M. Parrot, and J.-J. Berthelier (2012), Very-low-frequency saucers observed on DEMETER, *J. Geophys. Res.*, *117*, A09309, doi:10.1029/2012JA017965.

1. Introduction

[2] The spontaneous atmospheric whistler mode emission called the very-low-frequency (VLF) saucer continues to evoke scientific interest because it implies a peculiar source that remains small and fixed for seconds. These space and time scales are remarkably different from the scales associated with other wave-particle processes in the ionospheric-magnetospheric plasma [e.g., *LaBelle and Treumann*, 2002]. This localization and stability make saucers an attractive subject for study in a transient medium where it is typically difficult to examine a source of radio emission.

[3] Previous studies of VLF saucers provided the following evidence about their sources: (1) their spatial dimensions are in the 1- to 10-km scale size [*James*, 1976]; (2) they are located on lines of the earth's magnetic induction field $\mathbf{B_0}$ at auroral latitudes where downward conventional electrical current is carried by upward streaming electrons [*Gurnett and Frank*, 1972; *Lönnqvist et al.*, 1993; *Ergun et al.*, 2001, 2003]; (3) saucers are associated with double layers, solitary structures and electron phase-space holes [*Newman et al.*, 2002]; (4) the upward electron motion results in upward-propagating resonance-cone whistler mode (WM) waves through a two-stream instability [*Mosier and Gurnett*, 1969; *Gurnett and Frank*, 1972; *Newman et al.*, 2002]; (5) saucers are the resulting frequency-time (*f-t*) signatures in spectrograms from orbital receivers in a frequency range stretching from the lower-hybrid-resonance frequency f_{lh} at the satellite upward through the VLF part of the WM frequency range [*Smith*, 1969; *Mosier and Gurnett*, 1969; *James*, 1976].

[4] Comparatively recent observations of saucer spectrographic signatures [*Parrot et al.*, 2011] by the electric field instrument (Instrument Champ Electrique, ICE) [*Berthelier et al.*, 2006a] aboard the DEMETER spacecraft [*Parrot*, 2006] over its operational life, 2004–2010, have added new evidence about the nature of the highly localized sources of this quasielectrostatic WM radiation in the ionosphere. These relatively recent measurements warrant analysis because DEMETER orbited at altitudes around 660 km.

[5] This is significantly below the 1000–14000 km altitude range where older spacecraft recorded saucers [*Smith*, 1969; *Mosier and Gurnett*, 1969; *James*, 1976; *Lönnqvist et al.*, 1993; *Ergun et al.*, 2001]. Also, DEMETER data establish the existence of saucer sources in the dayside ionosphere.

[6] The conclusion of the present paper is that dayside saucer sources observed on DEMETER lie well above the observing satellite. This contrasts with previous papers, including that of *Parrot et al.* [2011], where the model is of upcoming radiation from sources below the satellite. Our conclusion that saucer sources radiate both up and down magnetic field lines is not completely surprising because the nonlinear two-stream instability predicts both upgoing and downgoing radiation from a source.

2. Basic Features of Saucers From DEMETER

[7] Although the DEMETER/ICE spectrograms show a variety of saucer-like hyperbolic *f-t* traces, some saucer frequency-time trace features are often repeated in the ICE data set. One such example is the spectrogram in Figure 1 of *Parrot et al.* [2011]. The authors point out the multiplicity of discrete hyperbolic traces. These imply localized sources at

[1]CRC, Ottawa, Ontario, Canada.
[2]LPC2E/CNRS, Orléans, France.
[3]Observatoire du Parc Saint-Maur, LATMOS/IPSL, Saint-Maur, France.

Corresponding author: H. G. James, CRC, Ottawa, ON K2H 8S2, Canada. (gordon.james@crc.ca)

0148-0227/12/2012JA017965

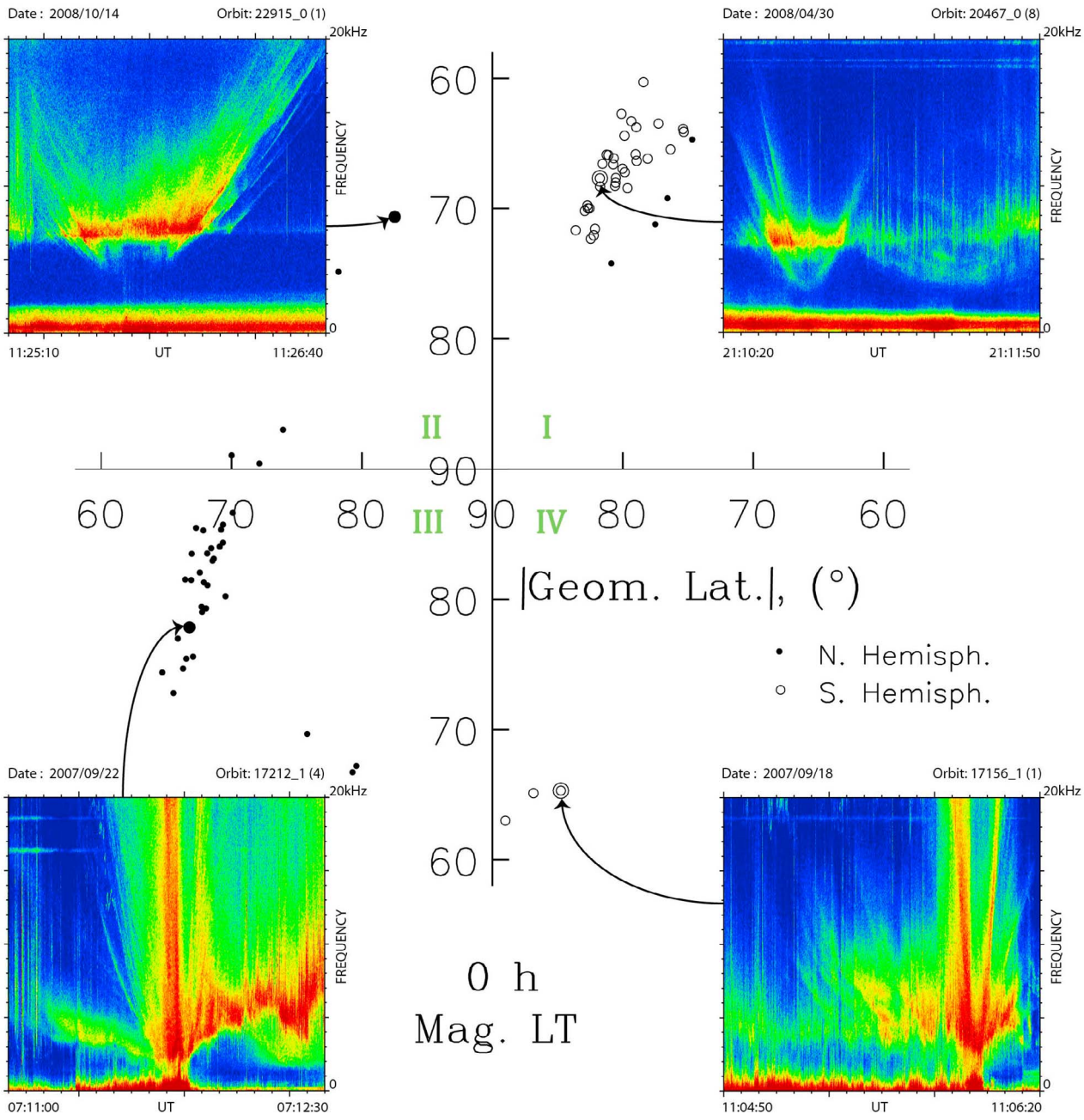

Figure 1. Distribution of saucer locations in magnetic local time and geomagnetic latitude, with spectrograms of typical saucers. Magnetic local time increases azimuthally in counterclockwise sense from 0 h at the bottom. The magnitude of the geomagnetic latitude decreases radially from 90° at the center of the plot.

different altitudes, some outside the orbital plane of the satellite. The strong lower limit of the main event ("truncation") from 09:55:00 to 09:55:46 around 6 kHz was interpreted under the assumption of sources below the spacecraft. As mentioned by these authors, whistler mode waves cannot propagate to the satellite when the open refractive index shape for $f > f_{lh}$ changes to a closed shape with comparatively small indices of refraction for $f < f_{lh}$. It will later be shown, however, that waves on the resonance cone can couple to propagation where $f < f_{lh}$.

[8] *Parrot et al.* [2011] stated that truncated saucers on DEMETER have their truncation frequency somewhat above the local f_{lh} determined solely from plasma measurements on the spacecraft. The present paper rather identifies the dayside saucer truncation frequency with the local f_{lh} and ascribes the difference in f_{lh} values between this assumption and the Parrot *et al.* method to the inherent limitations of the DEMETER plasma density measurements.

[9] Figure 1 of this paper is a polar diagram that summarizes typical shapes of saucers on DEMETER with

respect to geomagnetic latitude (radial distance) and magnetic local time (angle). Saucers were observed in both the north (closed circles) and south hemispheres (open circles). The locations were constrained by the local times of the sun-synchronous orbit (10 h, 22 h) and operational rules for scheduling of the spacecraft. In quadrants I and II of Figure 1 are seen typical examples of dayside saucers: f_{lh} lies near 6–7 kHz and intense noise appears near f_{lh} between the arms of the saucer. The opening of the arms is comparatively wide, implying comparatively large distances between the sources and the satellite.

[10] One of the findings in the ICE dayside data is the absence of clear, symmetric V-shaped traces continuously maintained through a range of frequencies starting upward from f_{lh}. Rather, the saucers recorded by DEMETER on the dayside often have the truncation signature of Parrot *et al.* As in their figure, the saucers in quadrants I and II of our Figure 1 imply a collection of sources on more or less the same field line: on the left side, straight arms of Vs appear, and on the right, the right half of Vs. These left and right sides may be interpreted as resulting from distant sources from which propagation separates the sides as seen at the spacecraft. Thus, in contrast to complete V-shaped saucers, there is apparently a difference between the narrow saucer sources observed by other satellites at, say, 2000 km altitude, that produce almost-complete Vs and this set of sources, at much different heights, that produce separated arms of Vs.

[11] V-shaped saucer arms dominate our dayside spectrograms in Figure 1, and imply source field lines close to each other and lying in the satellite orbital plane. The spectrogram of *Parrot et al.* [2011] also includes hyperbolic saucers whose minimal frequencies lie well above the truncation frequency of the main traces and whose sources are located on field lines to the side of the DEMETER orbital plane.

[12] The nightside saucers in quadrants III and IV of our Figure 1 have narrow opening angles and f_{lh} near 2 kHz. These relatively low f_{lh} values are reminiscent of the saucers previously observed at higher altitudes [*Smith*, 1969; *Mosier and Gurnett*, 1969; *Gurnett and Frank*, 1972; *James*, 1976]. The very steep strongest saucer arm at 07:11:48 in quadrant III also recalls the "VLF I" shape interpreted by *James* [1976] as the result of flight through a source where the spacecraft is thereby able to detect all source frequency components at once.

3. Estimation of Source Altitudes With Straight Rays

[13] The saucer data from the low-altitude DEMETER satellite re-open the question of whether the sources responsible are located above or below the spacecraft. First, we estimated the source-to-satellite height separations for Figure 1 of *Parrot et al.* [2011]. In our analysis, the knowledge of the electron density is critical to the calculation of resonance-cone angles, and hence in the determination of height separation. This analysis is supported by measurements at the spacecraft of the electron density, by the Langmuir probe (Instrument Sonde de Langmuir, ISL) [*Lebreton et al.*, 2006] and of the ion densities provided by the thermal ion analyzer instrument (Instrument d'Analyze du Plasma, IAP) [*Berthelier et al.*, 2006b].

[14] We use two different calculations to settle on a value of the electron plasma frequency f_{pe} at the spacecraft. Both approaches apply the relationship [*Smith and Brice*, 1964]

$$f_{pe} = \left[\frac{1}{\left(1/R_{eff}\, f_{lh}^2\right) - \left(1/f_{ce}^2\right)}\right]^{1/2} \tag{1}$$

involving f_{lh}, the electron gyrofrequency f_{ce}, and the ratio R_{eff} which equals 1836 times the effective ion mass. One computation simply uses the value of electron density measured by the ISL. During the interval 09:55:48–09:56:00, the ISL electron density corresponds to a plasma frequency of approximately 751 kHz. If we combine f_{lh} = 5 kHz found by *Parrot et al.*, f_{ce} = 626 kHz, and f_{pe} = 751 kHz in equation (1), we find R_{eff} = 9250, which is 1836 × 5.0. Hypothesizing that the ambient ion mixture contains only H^+ and O^+, an effective ion mass of 5 implies a mixture that is 88% O^+, which seems reasonable in the dayside ionosphere.

[15] The other computation evaluates f_{pe} from (1) taking again the measurement by Parrot *et al.* of f_{lh} = 5 kHz, f_{ce} = 626 kHz, but with O^+ ions only, making R_{eff} = 1836 × 16. This results in f_{pe} = 1284 kHz, which appears unduly large. Assuming, rather, an H^+-only plasma with R_{eff} = 1836 × 1 leads to the small value f_{pe} = 218 kHz. For discussion, we therefore accept the ISL measurement of f_{pe} = 751 kHz.

[16] Analysis of the frequency-time signatures of saucer traces begins with the fact that the half angle θ_k of the whistler mode wave number resonance cone is given by

$$\tan^2\,\theta_k = -\frac{P}{S}, \tag{2}$$

where S and P are functions of the frequency and plasma parameters in the cold-plasma dielectric tensor [*Stix*, 1992]. Since the group velocity for resonance-cone propagation lies at right angles to the wave vector, the half angle θ_g of the whistler mode group-velocity resonance cone obeys $\tan^2\,\theta_g = -S/P$. For the present analysis in which $f_{lh} < f \ll$ both f_{pe} and f_{ce}, angle θ_g obeys

$$\tan^2\,\theta_g \approx f^2\left(\frac{1}{f_{ce}^2} + \frac{1}{f_{pe}^2}\right) \equiv f^2 F_1^2. \tag{3}$$

As in *James* [1976], Figure 2 envisages the simplified geometry of straight rays and a source localized in all three dimensions. Anticipating findings below, orbital motion at velocity V_S takes the satellite through a field-aligned distance h below the source. At time $t = 0$ the spacecraft is at a minimum perpendicular separation x_0 from the magnetic field line through the source, so that we have

$$\tan\,\theta_g = \frac{x}{h} = \frac{\left(x_0^2 + V_S^2 t^2\right)^{1/2}}{h} = f F_1. \tag{4}$$

[17] To obtain first estimates of h, we assume that $f(t)$ can be scaled on the extremities of the saucer arms where $x_0^2 \ll V_S^2 t^2$, so that $df/dt = V_S/hF_1$. In Figure 1 by *Parrot et al.* [2011], in the interval 09:55:46–09:56:15 for frequencies between 10 and 20 kHz, one finds arm-extremity slopes of

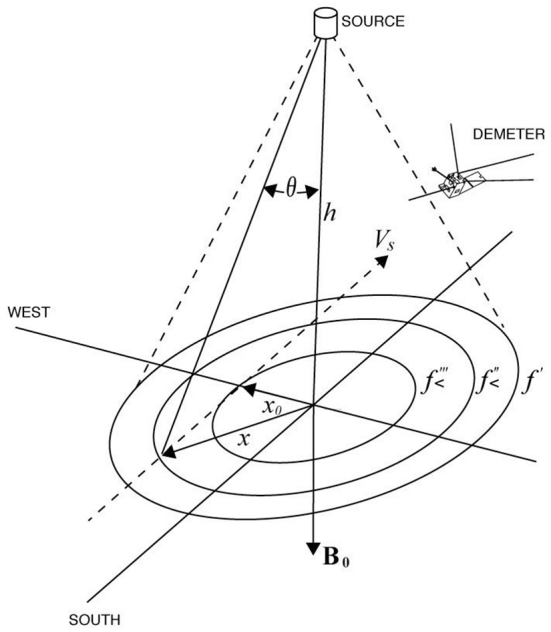

Figure 2. Geometry of the satellite track and the saucer radiation zone. The concentric rings labeled f''', f'' and f' identify group resonance cones at three different frequencies.

approximately 0.5 kHz s^{-1}. If f_{ce} = 626 kHz and f_{pe} = 751 kHz are inserted into F_1, and if the DEMETER orbital speed V_S = 7 km s^{-1}, $h = V_S(F_1\ df/dt)^{-1}$ = 6732 km. Because the plasma frequency at the spacecraft is higher than those measured on ISIS [*James*, 1976], the slope df/dt is much lower, and significantly greater values of the separation h result with DEMETER. These h magnitudes are much greater than the DEMETER satellite height. We infer that spectrogram slopes df/dt observed in dayside saucers require sources located above the spacecraft, as shown in Figure 2, but this requires detailed tests.

4. Source Altitudes Found With Ray Tracing

[18] The foregoing h values were estimated for a homogeneous ionosphere with straight rays. In this section we take account of refraction of the source-to-satellite rays for one nightside and two dayside saucers in Figure 1.

4.1. Nightside Case: Orbit 17156

[19] The interpretation of the saucer-arm slopes in this southern-hemisphere case begins by noting the similarity in the f-t shape of the main saucer to previously published examples from the high-latitude nightside ionosphere cited in section 2 above. Given such similarity, it was decided to first analyze the Orbit-17156 saucer as arising from a source below the satellite. The saucer is centered at 11:06:02, in the

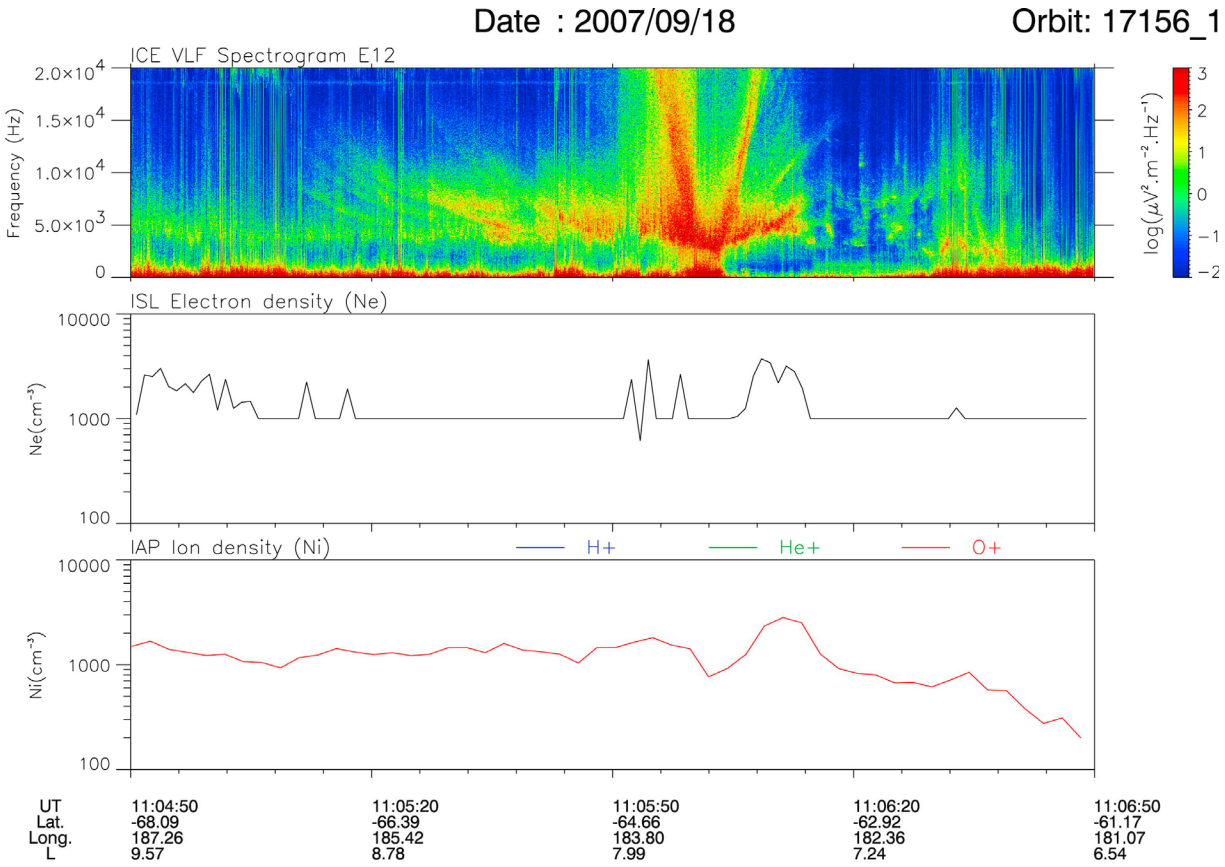

Figure 3. Data recorded by DEMETER on orbit 17156 on 18 September 2007. (top) ICE frequency-time spectrogram, shown also in quadrant IV of Figure 1; (middle) ISL electron density history; and (bottom) IAP oxygen-ion density history.

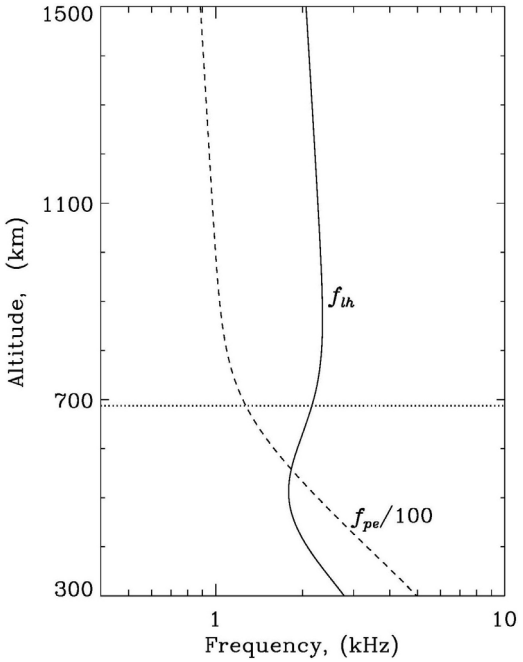

Figure 4. Altitude distributions $f_{pe}(y)$ and $f_{lh}(y)$ for the saucers of 18 Sept. 2007 in Figure 3, shown also in quadrant IV of Figure 1.

spectrograms in quadrant IV of Figure 1 and at the top of Figure 3. Local f_{lh} is at the apical point at about 2 kHz. In the middle and bottom of Figure 3 are also plotted electron density from the ISL and the oxygen-ion density from the IAP, respectively. As in previous nightside saucer observations, the plasma is tenuous, and electron density on the ISL is off-scale below 1000 cm^{-3}. Because of uncertainty about the precision of the displayed IAP density, it is assumed that the mixture of ions at the spacecraft altitude is 50% O^+ and 50% H^+, and we find the local electron density that provides f_{lh} = 2 kHz at DEMETER. In the absence of both measurements of, and theory for, the distributions with altitude y of the densities, the ionospheric diffusive-equilibrium density model of *Sonwalkar et al.* [2011a, 2011b] is used to extrapolate densities downward and upward from the satellite. With an equilibrium temperature of 1000 K at the spacecraft and a centered magnetic dipole model for predicting f_{ce}, the altitude distributions $f_{pe}(y)$ and $f_{lh}(y)$ are as in Figure 4.

[20] In Figure 4, one sees that $f_{lh}(y)$ has the expected doubly inflected shape as a function of y. Further, through equation (1), the value of f_{lh} = 2 kHz at DEMETER altitude (dotted line) constrains the plasma frequency to be $f_{pe} \sim$ 100–300 kHz in the topside ionosphere at and below the satellite. Consequently, resonance-cone rays traced upwards from below the spacecraft at the observed frequencies have group-velocity angles θ_g of no more than about 5°. Figure 5 is the result of a trial-and-error search to find a point-source altitude from which resonance-cone rays in the geomagnetic meridian produce *f-t* slopes that match the observed ones. Rays are traced here for f = 2.5, 3, 4, 5, 6, 8, 10, 12, 14, 16, 18, and 20 kHz. Starting wave normal directions, in region 8 of the Clemmow-Mullaly Allis (CMA) diagram [*Stix*, 1992], are chosen to assure resonance-cone propagation throughout CMA 8; this was done by requiring starting indices of refraction of the order of 100. Rays exhibit the expected slightly outward bend from the $\mathbf{B_0}$ line as the rising wave packets encounter decreasing electron densities. Wave propagation at all these frequencies remains in CMA region 8 close to the resonance cone for all ray positions between the source and the satellite altitude.

[21] Knowledge of the satellite velocity from ephemeris and of where the rising rays in Figure 5 intersect the satellite's orbital path has been converted to differential time. The resulting frequency-time traces are plotted in Figure 5 (inset). The continuous black lines overlaid on the spectrogram are the result of ray tracing from a stationary point source at an altitude of 400 km, as shown in the ray part of Figure 5. For this source altitude, the computed slopes of the saucers traces have good agreement with the observed traces. The uncertainty about ionospheric parameters precludes more careful parametrical studies to obtain better *f-t* agreement between observations and calculations.

[22] The concept of sources below the spacecraft, outlined in section 1 above, appears to be approximately borne out in this DEMETER nightside case. However, if we had opted to find a source altitude above the satellite that produces the same *f-t* slopes, the shapes of rays would be similar to those given in Figure 5, when rotated about the satellite position by 180° to place the source above the satellite. A somewhat lower satellite-source separation would be required because of the lower plasma density above the orbit. We also note that

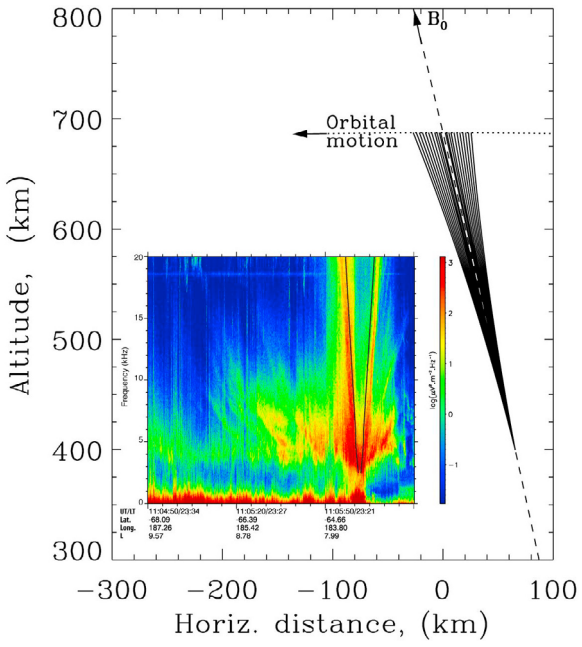

Figure 5. Rays traced in the magnetic meridian of the satellite for 2.5 ≤ f ≤ 20 kHz, for the saucers of 18 Sept. 2007 in Figure 3. The two 2.5-kHz rays lie closest to the field line through the source location at 400 km altitude. In the inset diagram, the resulting *f-t* plot is superposed in black lines on the spectrogram.

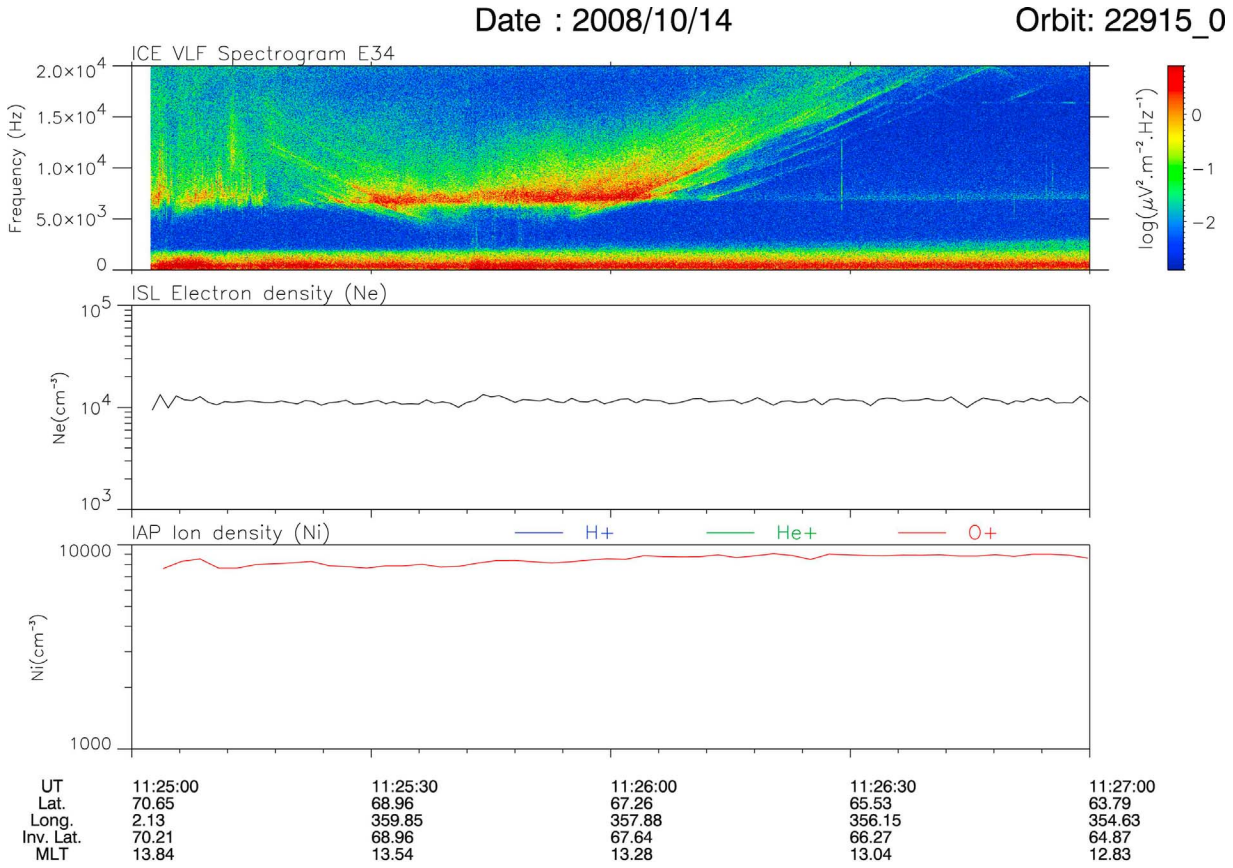

Figure 6. Data recorded by DEMETER on orbit 22915 starting at 11:25:00 on 14 October 2008. (top) ICE frequency-time spectrogram, shown also in quadrant II of Figure 1; (middle) ISL electron density history; and (bottom) IAP oxygen-ion density history.

the orbit-17156 spectrogram in Figures 1, 3 and 5 contains weaker saucer traces with significantly smaller *f-t* slopes than the traces analyzed. These traces imply sources at lower altitudes than 400 km. That sources could be triggered at such low altitudes in the collisional plasma near or below an assumed *F* region peak is doubtful. Whether nightside saucer sources usually lie on one side of the DEMETER satellite altitude remains an open question.

4.2. Dayside Cases: Orbits 22915 and 20467

[23] The orbit-22915 case depicted in quadrant II of Figure 1 was selected for detailed analysis, because it typifies the novel discovery on DEMETER of clear saucer-like phenomena in the Earth's dayside ionosphere. The ICE spectrogram and the in situ measurements of electron and oxygen-ion density are in Figure 6. Using the ISL-observed electron density of 10^4 cm^{-3}, f_{ce} = 1170 kHz from DEMETER ephemeris, f_{lh} = 6 kHz from the spectrogram and assuming that the ambient plasma mixture contains only protons and oxygen ions, based on equation (1) the mixture is found to be 7.1% H^+ and 92.9% O^+. The latter implied O^+ density is about 10% different from the IAP-measured value "Ni" in the bottom plot.

[24] Starting with the foregoing plasma parameters local to the satellite, diffusive-equilibrium models of density distributions of electrons and ions have been extended above and below the spacecraft using an equilibrium temperature of 1000 K. With a value of f_{pe} = 898 kHz at DEMETER and the assumption of even greater f_{pe} values below the satellite, values of the angle θ_g can be no more than several degrees at the observable frequencies. Ray tracing from sources below the spacecraft then yields very steep saucer arms in *f-t*, much steeper than the observed ones. The inescapable conclusion is that the dayside saucer sources are above DEMETER where comparatively low f_{pe} values and comparatively large source-satellite distances can produce comparatively low *f-t* arm slopes in spectrograms at DEMETER's orbital altitude.

[25] The truncation form of dayside saucers in the DEMETER/ICE spectrograms reported by *Parrot et al.* [2011] is seen in the dayside saucers of our Figure 1. From the ensemble of DEMETER dayside saucer spectrograms that have been gathered, it is found that the truncation of saucer arms at the putative f_{lh} is not sharp. Rather, in some cases the arms extend for a fraction of 1 kHz to frequencies below f_{lh}.

[26] The quadrant-I spectrogram in Figure 1 (Orbit 20467) contains saucer traces that serve as an illuminating example of truncation. Straight saucer arms are seen extending upwards from both sides of a region of partial truncation. The arms are not completely cut off at the ostensible $f_{lh} \approx 6$ kHz but rather continue down to lower frequencies and almost join at about $f = 3$ kHz. We infer that a saucer source has

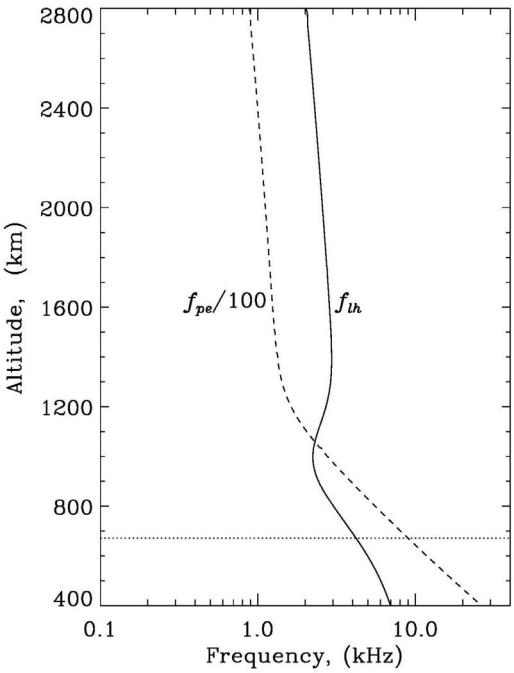

Figure 7. Altitude distributions $f_{pe}(y)$ and $f_{lh}(y)$ for the saucers of 14 October 2008 in Figure 6, shown also in quadrant II of Figure 1.

been able to create WM radiation at frequencies above 3 kHz. Our interpretation is that the source(s) are above the satellite, and have created downward resonance-cone whistler mode waves throughout $3 < f < 16$ kHz. The sequence of propagation conditions is not unlike that of classical descending whistler spectral components when they encounter the lower-hybrid resonance condition, with the qualification that we deal here with WM propagation on or near the resonance cone. We conceive this sequence to be like that of the top three refractive-index surfaces of Figure 4b of *Sonwalkar et al.* [2011b]. The waves are created at the top of this diagram through some wave instability made possible by the large refractive-index values on the resonance cone surface. The waves start downward, propagating in CMA region 8 near the resonance cone. As density increases, the group resonance cone angle narrows and rays become more nearly parallel. Eventually waves at comparatively low frequencies f encounter the altitude where $f = f_{lh}$. These waves convert to a closed refractive surface and continue downward, arriving at the satellite with a CMA-region-11 refractive index curve. Higher frequencies remain in CMA 8 all the way to the satellite.

[27] Returning to the Orbit-22915 case, the electron and ion altitude distributions from the method of *Sonwalkar et al.* [2011b] were therefore constrained to have $f_{lh} = 2$–3 kHz at the superior source altitude, in addition to the parameter values already listed. This was achieved, in part, through the use of the 1000 K temperature at the satellite where the IAP actually measured an ion temperature of 1300 K. Saucer signatures similar to some of those observed were found, by a process of trial and error, with a source altitude of 2800 km. Profiles of $f_{pe}(y)$ and $f_{lh}(y)$ are plotted in Figure 7, while the raypaths and corresponding *f-t* spectrogram fit are in Figure 8. The frequencies plotted are 3, 3.5, 4, 4.5, 5, 6, 7, 8, 10, 12, 14, 16, 18, and 20 kHz, the lower limit being just above the local f_{lh} at the source. It is seen that the predicted *f-t* traces in continuous white line resemble some of the observed ones. We deduce from the magnitudes of the slopes of dayside saucers arms that their sources lie well above the DEMETER spacecraft.

[28] Figure 9 displays cold-plasma refractive index surfaces for three ray frequencies of interest for Figure 8. Each panel shows the surfaces at four different altitudes between the source at 2800 km and the altitude of 700 km just above DEMETER. We plot the surfaces on a common *x-y* origin, whereas *Sonwalkar et al.* [2011b, Figure 4b] spaced them out. The frequencies of 2.5, 3.5 and 5 kHz chosen for inclusion in Figure 9 represent three relevant sequences through the CMA diagram. Poeverlein's construction [*Budden*, 1985] is the basis for the following discussion, wherein we assume that the perpendicular component of the refractive index is conserved as a wave packet encounters different refractive-index surfaces on its way from the source to the satellite.

[29] 2.5-kHz waves start out as resonance-cone propagation just above f_{lh} at the source but convert to CMA 11 around 1800 km. The maximum refractive index value in dotted line for 1400 km is comparatively small. In fact, waves at 2.5 kHz reflect at a somewhat greater altitude. The gap at the bottom of the superposed white saucer trace in Figure 8 appears because the frequencies needed to close that gap are prevented by reflection from reaching the satellite.

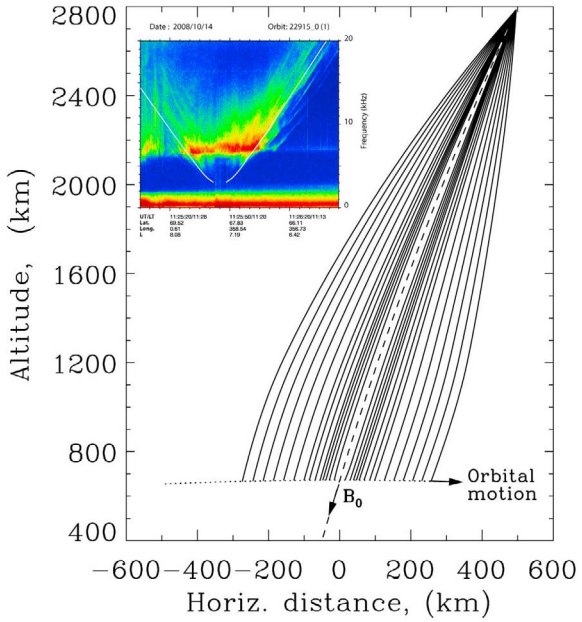

Figure 8. Rays traced in the magnetic meridian of the satellite for $3 \le f \le 20$ kHz, for the saucers of 14 October 2008 in Figure 6. The two 3-kHz rays lie closest to the field line through the source location at 2800 km altitude. In the inset diagram, the resulting *f-t* plot is superposed in white lines on the spectrogram.

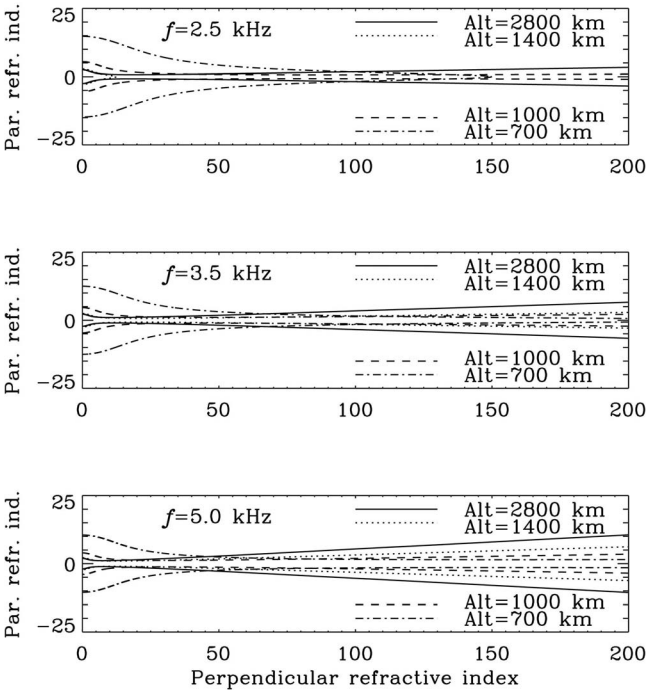

Figure 9. Cold-plasma refractive-index surfaces for waves at frequencies f propagating from a source altitude at 2800 km down to satellite altitude, for the saucers of 14 October 2008 in Figure 6.

[30] Waves at 3.5 kHz remain in resonance-cone propagation until an altitude of about 750 km. There they can couple directly to CMA-11 propagation and so continue to the satellite because the CMA-11 surface has large values along the x axis matching those in CMA 8. See the curve for 700 km altitude in dot-dash line in the middle panel.

[31] Waves at 5 kHz encounter values of f_{lh} that remain less than 5 kHz throughout the raypath between the source and spacecraft and so remain in CMA-8 resonance-cone propagation to the satellite.

[32] The comparatively indistinct, ghostly character of dayside saucer arms below local f_{lh}, and their incompleteness in our Figure 1 and elsewhere in DEMETER data, may indicate that not all the incident wave spectrum does succeed in being converted to the closed refractive surface to continue downward. Rather, some of the wave number (k) spectrum may be reflected back upwards. The fact that some DEMETER saucer arms have sharp lower edges but comparatively diffuse upper edges indicates that these saucers are carried by a spectrum of wave numbers at each frequency. Whether such spectral width results from the nature of the creative instability in the localized source, or rather arises from subsequent scattering as the waves encounter density irregularities [*Sonwalkar et al.*, 2011a] remains for separate investigation.

[33] It is to be noted that the theory of diffusive equilibrium has been "borrowed" as a convenient way to model the altitude distributions of electrons and ions. Diffusive equilibrium is difficult to prove, given nonequilibrium high-latitude features such as electric fields and electron streams associated with saucers. The temperature applied to the *Sonwalkar et al.* [2011b] density expressions was adjusted to provide the reasonable altitude distributions in Figure 7 that are consistent with important features of the 22915 spectrogram in Figures 1, 6 and 8: f_{lh} at the satellite and minimal frequency equal to f_{lh} at the source.

5. Other Indications of Down-Coming Saucer Propagation

[34] An enlarged version of the spectrogram in quadrant III of Figure 1 has been reproduced in Figure 10, which clearly shows periodic attenuation bands, in $3 < f < 7$ kHz. Similar to the data of *Horita and James* [1982] and *Corcuff and Tixier* [1985], the periodicity here is very close to the proton gyrofrequency at the observing spacecraft. *Horita and James* [1982] concluded that the periodicity at ISIS II (altitude 1400 km) implied downcoming waves because most of their scaled values of periodicity were smaller than the proton gyrofrequency at that satellite.

[35] The periodicity in Figure 10 is evaluated to be 600 ± 30 Hz. The proton gyrofrequency at DEMETER according to the IGRF real field model for the date is 635.5 Hz. There is therefore little difference between the proton gyrofrequency at DEMETER and the observed periodicity. In Figure 10, the steepness of the almost-vertical saucer arm at 07:11:48 also implies a source close in altitude to DEMETER There are few other clear examples of

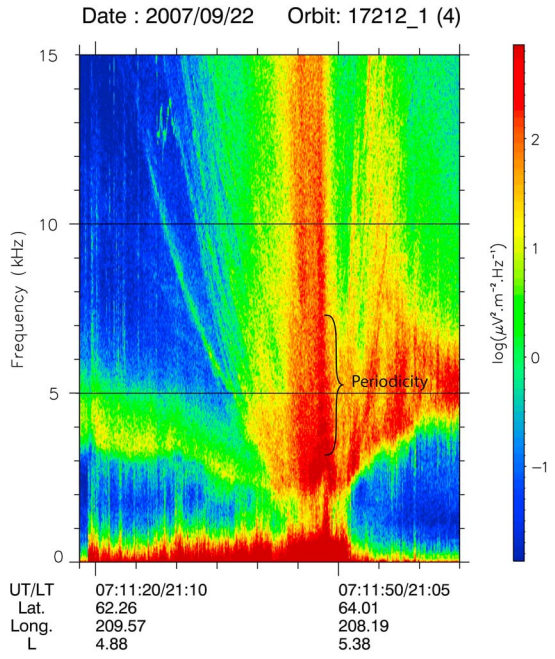

Figure 10. Enlargement of the ICE spectrogram in quadrant III of Figure 1. Periodic modulation of the spectrum is seen in the frequency range $3 \leq f \leq 7$ kHz, with a periodicity close to the proton gyrofrequency.

putative gyrofrequency periodicity in the DEMETER saucers found so far.

[36] *Gurnett and Frank* [1972, Plates 4 and 5] published saucer-like spectrogram traces whose propagation directions, determined using wave electric and magnetic field measurements, indicated downward propagation, unlike the upward directions of saucers appearing on the same spectrograms.

6. Saucer Source Mechanism

[37] The observed collocation of magnetic flux tubes containing sources and upgoing electron fluxes [*Lönnqvist et al.*, 1993; *Ergun et al.*, 2001] prompted the examination of the nonlinear theory of two-stream instability as a candidate explanation for saucers. The upgoing electron beam, providing downward magnetospheric current, constitutes one stream and the background electrons at rest at the source the other. Nonlinear growth of whistler mode waves creates vortices of trapped particles in phase space known as "holes." Various observations in the magnetosphere of "bipolar solitary structures" are interpreted in terms electron phase-space holes [*Oppenheim et al.*, 2001; *Ergun et al.*, 2001].

[38] *Goldman et al.* [1999] and *Oppenheim et al.* [2001] computed the evolution of a double-peaked electron distribution to a late-time merged nonthermal distribution. They assumed f_{ce}/f_{pe} = 5 and equal beam and background f_{pe} values. On time scales as large as about $1000/f_{pe}$ the vortices develop then decay, transferring energy to quasi-electrostatic whistler mode waves which are observable as saucers.

[39] Saucer observations support some of the features of the two-stream simulations. First, we note that a beam-plasma linear instability condition $\omega = k_B V_b$ involving wave angular frequency ω, **k**-vector component k_B parallel to $\mathbf{B_0}$ and monoenergetic beam velocity V_b, requires frequencies of at least 10 kHz, well above f_{lh}, for an observed upward electron beam speed V_b corresponding to 10 eV. The detection of strong saucer radiation right down to local f_{lh} appears to require the nonlinear decay of holes into broadband whistler mode saucer noise as appears in the simulations. Second, in both the 2D simulation of *Goldman et al.* [1999] and the 3D simulation of *Oppenheim et al.* [2001], the nonlinear whistler mode power spectrum resulting from the nonlinear decay has equal levels in the beamward and anti-beamward directions. This particular finding of the bidirectional shape of the saucer radiation pattern explains the inferences from DEMETER and earlier spacecraft of down coming waves.

[40] A third observation has to do with the presence of hiss-like noise near f_{lh}. As can be seen in the spectrograms of Figure 1, between the arms of dayside saucers there is typically intense noise stretching from around f_{lh} upwards by a few kilohertz. Outside the arms the noise is seen at earlier and later times but at considerably lower intensities. The simulations by *Oppenheim et al.* [2001] show that a 3D approach favors flow of energy from whistler mode to lower-hybrid-mode waves.

[41] Fourthly, the $\mathbf{B_0}$-aligned extent of a localized acceleration region can be estimated as $(1000/f_{pe})V_b \approx 20$ km for 10-eV electrons and f_{pe} = 90 kHz at the source altitude of 2800 km in Figure 8. This source-length estimate roughly agrees with the 10-km value scaled by *James* [1976] from ISIS spectrograms.

7. Geophysical Conditions for the Existence of Sources

[42] The kinetic theory for ES whistler mode waves arising from the formation and decay of phase-space holes supplies a model for microscale plasma physics of saucers. This nonlinear kinetic theory predicts lifetimes of the order of $1000/f_{pe}$ [*Ergun et al.*, 2001], which in our dayside case of Figure 7 is about 10 ms. Observations and analyses have left unanswered the question of why or how localized, stationary sources can persist for about 10 s. The dayside saucers on DEMETER are composite events lasting the order of 1 min and often arising from a group of closely located but separate sources, sometimes short-lived given the discontinuity of some arms. "Fast solitary waves" [*Ergun et al.*, 1998, and references therein] are bipolar localized structures in the downward current region but are not stationary for seconds; rather they are thought to move upward at speeds like those of the electron streams under discussion. Double layers are attractive as a concept for providing upward acceleration of electrons in sources, but, again are not stationary and have lifetimes much shorter than saucer sources [*Singh et al.*, 2009].

[43] In the three-dimensionally localized source implicit in equation (4), the nonzero separation x_0 is retained to explain hyperbolic saucers that are detected when the observer passes to the east or to the west of the source field line. *Temerin* [1979] demonstrated that line sources localized only in two dimensions can produce saucer spectra that are similar in satellite spectrograms to those produced with a 3D-localized source. Furthermore, the hyperbolic signature could be produced by a sharp bend in an auroral-arc-associated line source. The line source hypothesis becomes less tenable given the common appearance of discrete, hyperbolic saucers in DEMETER spectrograms from the dayside, where auroral arcs are rarely continuous lines with sharp bends.

[44] The development of auroral dynamic concepts has proposed that Alfven waves in the ionospheric Alfven resonator (IAR) can produce small-scale density and current structure in the downward current region of the ionosphere [e.g., *Streltsov and Lotko*, 2008]. Such structures have their roots in the low ionosphere but stretch upward through the altitudes of saucer sources. Shear Alfven waves have frequencies of 0.1–1 Hz, and a pulse of such waves can act nonlinearly to produce the structure. There is some consistency in the time scale of action (100 s) and the 10-s existence of saucer sources. Simulations by *Sydorenko et al.* [2010] show, on time scales of 100 s after entry of an SAW packet into the IAR, that ponderomotive forces of the first-harmonic standing SAW pattern produce a large enhancement in topside ambient electron density and a separate, higher depletion. These lead to the formation of spikes of electric field as a function of altitude and then to sharpened ion-acoustic waves that resemble double layers. However, such features are not stationary. Furthermore the potential drops across the layers are insufficient for the

creation of saucer-causing streams. So far, the analysis of observations leaves unsolved the conundrum of the stationary, small source.

[45] In the context of cavities, *Knudsen et al.* [2012] have discussed a model of field-aligned filamentary density cavities through which upgoing electrons stream, based on observations from the "GEODESIC" rocket experiment. These authors consider that such "lower hybrid solitary structures" may exist in saucer sources. Based on observations, the perpendicular dimension of a cavity is thought to be determined by ion dynamics [*Knudsen et al.*, 2004]. Their model sets the time scale for the growth of cavities that participate in the generation of saucer waves to an ion gyroperiod. It is intriguing to find a strong band of lower-hybrid hiss between the arms of the DEMETER dayside saucers. Lower-hybrid resonance waves are predicted in the two-stream theory [*Oppenheim et al.*, 2001]. Some of the same GEODESIC observations relate to physical scales of interest: a discrete negative pulse on the Kaktovik magnetometer on the ground underneath the rocket trajectory lasted about 100 s, a time predicted (above) for the nonlinear action of a shear Alfvén wave; also a system of currents structured on saucer-like scales of kilometers were identified as the region of downward return current.

[46] As regards future measurements that may throw further light on the nature of saucers, we note that the upcoming launch of the CASSIOPE spacecraft will place in high-inclination low-earth orbit the Enhanced Polar Outflow Probe (e-POP) suite of instruments [*Yau and James*, 2011]. These include electron and ion, low-energy, two-dimensional spectrometers and a radio receiver. The perigee and apogee of CASSIOPE/e-POP, 325 and 1500 km respectively, bracket the orbital altitude of DEMETER, which indicates that e-POP should be able to observe saucer sources at close range, particularly on the nightside.

8. Conclusions

[47] DEMETER recorded saucers at altitudes around 660 km in both hemispheres, on both the dayside and nightside. Rays traced in the quasi-electrostatic whistler mode strongly imply that the dayside sources are located above the satellite. Continuing the assumption that saucers are fed by up-streaming, low-energy electrons, we are led to the conclusion that saucer sources radiate both parallel and antiparallel to $\mathbf{B_0}$. Such bidirectional radiation is predicted by the nonlinear theory of the two-stream instability. The present interpretation of down-coming saucer radiation is supported by previous evidence.

[48] This analysis of DEMETER observations leaves unresolved particular challenges in the geophysics of saucers. It remains to explain how a two-stream instability can persist for several seconds in one location. Time and space scales of structures appearing in the ionospheric Alfvén resonator predicted by models of shear Alfvén waves may promise eventual explanations of saucer sources.

[49] **Acknowledgments.** The authors are grateful to Vikas Sonwalkar for sharing ray-tracing computer code and associated programs for electron and ion density distributions as a function of altitude. The work of M.P. and J.J.B. was supported by the Centre National d'Etudes Spatiales (CNES). This paper is mainly based on observations with the electric field experiment ICE embarked on DEMETER.

[50] Robert Lysak thanks the reviewers for their assistance in evaluating this paper.

References

Berthelier, J.-J., et al. (2006a), ICE, the electric field experiment on DEMETER, *Planet. Space Sci.*, *54*, 456–471, doi:10.1016/j.pss.2005.10.016.

Berthelier, J.-J., M. Godefroy, F. Leblanc, E. Seran, D. Peschard, P. Gilbert, and J. Artru (2006b), IAP, the thermal plasma analyzer on DEMETER, *Planet. Space Sci.*, *54*, 487–501, doi:10.1016/j.pss.2005.10.018.

Budden, K. G. (1985), *The Propagation of Radio Waves: The Theory of Radio Waves of Low Power in the Ionosphere and Magnetosphere*, Cambridge Univ. Press, Cambridge, U. K., doi:10.1017/CBO9780511564321.

Corcuff, Y., and M. Tixier (1985), VLF saucers with attenuation bands, in *Results of the ARCAD 3 Project and of Recent Programs in Magnetospheric and Ionospheric Physics*, *Rep. N87-10541 01-46*, pp. 529–535, Cepadues Ed., Toulouse, France.

Ergun, R. E., et al. (1998), FAST satellite observations of large amplitude solitary structures, *Geophys. Res. Lett.*, *25*(12), 2041–2044, doi:10.1029/98GL00636.

Ergun, R. E., C. W. Carlson, J. P. McFadden, R. J. Strangeway, M. V. Goldman, and D. L. Newman (2001), Electron phase-space holes and the VLF saucer source region, *Geophys. Res. Lett.*, *28*, 3805–3808, doi:10.1029/2001GL013024.

Ergun, R. E., C. W. Carlson, J. P. McFadden, R. J. Strangeway, M. V. Goldman, and D. L. Newman (2003), FAST observations of VLF saucers, *Phys. Plasmas*, *10*, 454–462, doi:10.1063/1.1530160.

Goldman, M. V., M. M. Oppenheim, and D. L. Newman (1999), Nonlinear two-stream instabilities as an explanation for auroral bipolar structures, *Geophys. Res. Lett.*, *26*, 1821–1824, doi:10.1029/1999GL900435.

Gurnett, D. A., and L. A. Frank (1972), VLF hiss and related plasma observations in the polar magnetosphere, *J. Geophys. Res.*, *77*, 172–190, doi:10.1029/JA077i001p00172.

Horita, R. E., and H. G. James (1982), Source regions deduced from attenuation bands in VLF saucers, *J. Geophys. Res.*, *87*, 9147–9153, doi:10.1029/JA087iA11p09147.

James, H. G. (1976), VLF saucers, *J. Geophys. Res.*, *81*, 501–514, doi:10.1029/JA081i004p00501.

Knudsen, D. J., et al. (2004), Lower-hybrid cavity density depletions as a result of transverse ion acceleration localized on the gyroradius scale, *J. Geophys. Res.*, *109*, A04212, doi:10.1029/2003JA010089.

Knudsen, D. J., R. Kabirzadeh, J. K. Burchill, R. F. Pfaff, D. D. Wallis, S. R. Bounds, J. H. Clemmons, and J.-L. Pinçon (2012), Strong magnetic field fluctuations within filamentary auroral density cavities interpreted as VLF saucer sources, *J. Geophys. Res.*, *117*, A02217, doi:10.1029/2011JA017316.

LaBelle, J., and R. A. Treumann (2002), Auroral radio emissions, 1. Hisses, roars, and bursts, *Space Sci. Rev.*, *101*, 295–440, doi:10.1023/A:1020850022070.

Lebreton, J.-P., et al. (2006), The ISL Langmuir probe experiment processing onboard DEMETER: Scientific objectives, description and first results, *Planet. Space Sci.*, *54*, 472–486, doi:10.1016/j.pss.2005.10.017.

Lönnqvist, H., M. André, L. Matson, A. Bahnsen, L. G. Blomberg, and R. E. Erlandson (1993), Generation of VLF saucer emissions observed by the Viking satellite, *J. Geophys. Res.*, *98*(A8), 13,565–13,574, doi:10.1029/93JA00639.

Mosier, S. R., and D. A. Gurnett (1969), VLF measurements of the Poynting flux along the geomagnetic field line with the Injun 5 satellite, *J. Geophys. Res.*, *74*, 5675–5687, doi:10.1029/JA074i024p05675.

Newman, D. L., M. V. Goldman, and R. E. Ergun (2002), Evidence for correlated double layers, bipolar structures, and VLF saucer generation in the auroral ionosphere, *Phys. Plasmas*, *9*, 2337–2343, doi:10.1063/1.1455004.

Oppenheim, M. M., G. Vetoulis, D. L. Newman, and M. V. Goldman (2001), Evolution of electron phase-space holes in 3D, *Geophys. Res. Lett.*, *28*, 1891–1894, doi:10.1029/2000GL012383.

Parrot, M. (2006), *First Results of the DEMETER Micro-satellite*, *Planet. Space Sci.*, vol. 54, Elsevier, Amsterdam.

Parrot, M., J.-J. Berthelier, and J.-Y. Brochot (2011), Truncated VLF saucers observed by the low altitude satellite DEMETER, *IEEE Trans. Plasma Sci.*, *39*(11), 2702–2703, doi:10.1109/TPS.2011.2131682.

Singh, N., K. Arcot, and B. E. Wells (2009), Parallel electric fields in mixing hot and cold plasmas in the auroral downward current region: Double layers and ambipolar fields, *J. Geophys. Res.*, *114*, A03209, doi:10.1029/2008JA013591.

Smith, R. L. (1969), VLF observations of auroral beams as sources of a class of emissions, *Nature*, *224*, 351–352, doi:10.1038/224351a0.

Smith, R. L., and N. Brice (1964), Propagation in multicomponent plasmas, *J. Geophys. Res.*, *69*, 5029–5040, doi:10.1029/JZ069i023p05029.

Sonwalkar, V. S., D. L. Carpenter, A. Reddy, R. Proddaturi, S. Hazra, K. Mayank, and B. W. Reinisch (2011a), Magnetospherically reflected, specularly reflected, and backscattered whistler mode radio-sounder echoes observed on the IMAGE satellite: 1. Observations and interpretation, *J. Geophys. Res.*, *116*, A11210, doi:10.1029/2011JA016759.

Sonwalkar, V. S., A. Reddy, and D. L. Carpenter (2011b), Magnetospherically reflected, specularly reflected, and backscattered whistler mode radio-sounder echoes observed on the IMAGE satellite: 2. Sounding of electron density, ion effective mass (m_{eff}), ion composition (H^+, He^+, O^+), and density irregularities along the geomagnetic field line, *J. Geophys. Res.*, *116*, A11211, doi:10.1029/2011JA016760.

Stix, T. H. (1992), *Waves in Plasmas*, Am. Inst. of Phys., New York.

Streltsov, A. V., and W. Lotko (2008), Coupling between density structures, electromagnetic waves and ionospheric feedback in the auroral zone, *J. Geophys. Res.*, *113*, A05212, doi:10.1029/2007JA012594.

Sydorenko, D., R. Rankin, and K. Kabin (2010), Excitation and steepening of ion-acoustic waves in the ionospheric Alfvén resonator, *J. Geophys. Res.*, *115*, A11212, doi:10.1029/2010JA015448.

Temerin, M. (1979), A comment on the source region of VLF saucers, *J. Geophys. Res.*, *84*(A11), 6691–6693, doi:10.1029/JA084iA11p06691.

Yau, A. W., and H. G. James (2011), Scientific objectives of the Canadian CASSIOPE Enhanced Polar Outflow Probe (e-POP) small satellite mission, in *The Sun, the Solar Wind, and the Heliosphere*, *IAGA Spec. Sopron Book Ser.*, vol. 4, edited by M. P. Miralles and J. Sanchez Almeida, pp. 355–364, Springer, Dordrecht, Netherlands, doi:10.1007/978-90-481-9787-3.